SAM LGS system (overview)

Prepared by: *A. Tokovinin*
Revised by: *B. Gregory*
Version: 2.2
Date: August 20, 2007
File: soar/laser/pdr/samlgs.tex

1 Introduction

The SOAR Adaptive Module (SAM) is an adaptive optics system designed to correct wavefront distortions due to low-altitude turbulence and thereby to improve the image quality in a relatively wide field-of-view at visible wavelengths (Ground-layer adaptive optics, GLAO). SAM will measure wavefront distortions using an artificial laser guide star (LGS) created by scattering in the low atmosphere (Rayleigh LGS). The concept of SAM is described in [6, 8]. Extensive technical material is available at the project web site.[1]

In this document, an overview of the SAM LGS sub-system will be given. For convenience, major parameters of SAM are listed in the Table 1. The SOAR telescope is described in [3].

Table 1: SAM: major instrument parameters

Sub-system	Description
Deformable mirror	Bimorph BIM-60 (Cilas), pupil 50mm, 60 electrodes
Wave-front sensor	Shack-Hartmann 10x10, CCD-39, $0\farcs37$ pixels in $3\farcs0$ sub-apertures
Re-imaging optics	Two OAPs $F = 810$ mm, off-axis shift 213.3 mm
Laser	Tripled Nd:YAG, $\lambda = 355$ nm, 10W, 10 kHz
Laser Launch Telescope	$D = 0.3$ m, reflecting, behind the SOAR secondary, $H = 7...14$ km
Range gating	KD*P longitudinal Pockels Cell + two $\lambda/4$ plates and polarizers
Tip-tilt guiding	Two probes linked by fibers to APDs, $R_{lim} = 18$
Focal plane	$3'$x$3'$ square field, $f/16.5$, scale 3 arcsec/mm, $R_{curv} = -0.9$m
CCD imager	4Kx4K, $0\farcs05$ pixels, 6 filters
Collimated space	50-mm beam, 75 mm along axis (ADC, user filter)

Our goal is to design a low-cost instrument which will be easy to operate and maintain. Ideally, the SAM LGS must be a "set-and-forget" system. This leads us to adopt commercial and standard solutions as much as possible. This strategy influenced several decisions discussed below. The requirements for the SAM LGS are listed in [16] and follow from the general requirements for SAM [9].

[1] `http://www.ctio.noao.edu/new/Telescopes/SOAR/Instruments/SAM/`

2 Rayleigh LGS at SAM and elsewhere

2.1 SAM LGS

Most astronomical AO systems use sodium LGS produced by fluorescence of Na atoms at ∼90 km altitude. High altitude is sought to reduce the cone effect. In SAM, we intentionally place the LGS at low altitude to increase the cone effect, and thus to achieve selective sensing of ground-layer turbulence and therefore relatively wide-field correction. The LGS is created by Rayleigh scattering from the air molecules and Mie scattering from aerosols.

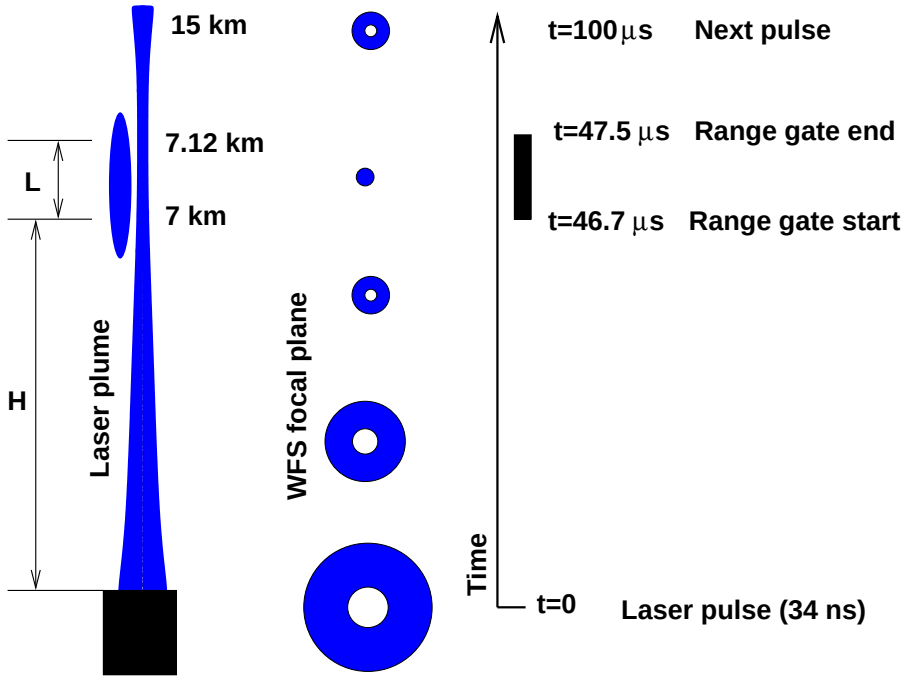

Figure 1: Propagation of the laser pulse ("bullet") in the atmosphere and range-gating. The "donuts" depict defocused images of the laser spot in the wave-front sensor (WFS) at different moments.

Figure 1 illustrates the Rayleigh LGS concept as implemented in SAM. A short (dt = 34 ns) laser pulse propagates upwards, launched from a 30-cm telescope (laser launch telescope, LLT). The apparent vertical extent of the light bullet is $dH = dt\ c/2 = 5$ m (including the round-trip time which effectively reduces the speed of light 2 times). After 46.7 μs the scattered light the bullet has reached the distance of 7 km and the scattered light has traveled back. When the back-scattered light reaches the wavefront sensor (WFS), we open the fast shutter in the WFS and accumulate photons during a *range gate* time of 0.8 μs. This time corresponds to the vertical LGS extent of 120 m to keep it within the "focus depth" of the SOAR telescope. The range gate duration is selected to balance several conflicting factors (see below).

The delay t between the emission of the laser pulse and the middle of the shutter exposure is $t = 2H/c$ for the LGS distance (range) H, where $c = 3\ 10^8$ m/s is the speed of light. The time the shutter is open is $\Delta t = 2L/c$, where L is the vertical extent of the LGS which depends on the altitude

H and the maximum permitted spot elongation α, $L = H^2\alpha/R$. Here $R = 2$ m is the distance of the outer sub-aperture from the optical axis (in fact the LLT axis). Representative numbers are given in Table 2.

Table 2: Shutter delay and range gate timings

H, km	t, μs	$L(1'')$, m	$\Delta t(1'')$, μs
7	46.7	119	0.79
10	66.7	242	1.61
14	93.3	475	3.17

The optics of the WFS are focused at the distance of 7 km. During the period when the range gate is opened, the image of the laser spot is sharp. Before or after that, the spot is strongly defocused. Defocus actually helps to block the light scattered at other altitudes because the WFS entrance aperture falls into the shadow of the SOAR central obscuration. Thus, strong light scattered from low altitudes does not enter the WFS even without any range gating. It is important to place the LLT at the center, behind the SOAR M2 mirror, to minimize the spot elongation in the WFS and to block the low-altitude scattering.

Laser pulses repeat with a frequency of $\nu_{PRF} = 10$ kHz. When the next pulse is emitted, the radiation from the previous pulse is already detected from the altitude of 15 km where the scattered light is faint and defocused. By setting low LGS altitude, the system can work at a higher pulse frequency (and low pulse energy) and use robust commercial lasers. We can operate SAM with $\nu_{PRF} \leq 20$ kHz if $H = 7$ km.

SAM will use a frequency-tripled Nd:YAG laser emitting at 355 nm wavelength. This UV radiation is not visible (no visual hazards to aircraft) and easily separated from the science photons with longer wavelengths. Moreover, the number of photons from Rayleigh scattering is proportional to λ^{-3}, favoring the UV.

2.2 Other astronomical Rayleigh LGS systems

The Ground-Layer Laser Adaptive Optics System (GLAS) is being built for the 4.2-m William Hershel Telescope at La Palma [5]. It will also use a Rayleigh LGS, but placed at 25 km to achieve higher compensation in a smaller field. This choice requires a more powerful (25W) laser with low $\nu_{PRF} =$ 5 kHz, so the GLAS laser is a custom frequency-doubled Nd:YAG laser. Filtering the green 532 nm radiation from the science channel requires special attention. The GLAS system has seen its first laser light on May 27, 2007.

The Multi-Mirror Telescope (MMT) at Mt. Hopkins is equipped with an LGS system projecting 5 green spots at 532 nm at altitudes up to 30 km [1]. This LGS provides for both turbulence tomography (to beat the cone effect) and GLAO. Two 12-W Nd:YAG frequency-doubled industrial lasers with $\nu_{PRF} = 5$ kHz are combined with a polarization beam-splitter and the beam is sent to a 50-cm LLT, where it is split into 5 beams by a hologram (Fig. 2). We visited the MMT LGS facility on April 16, 2006. Several aspects of this successful system are copied by SAM.

Both GLAS and MMT have LLTs with 50-cm refractive optics. The optimum size of the LLT aperture is proportional to the wavelength, so the 30-cm SAM LLT matches the 50-cm LLTs used in

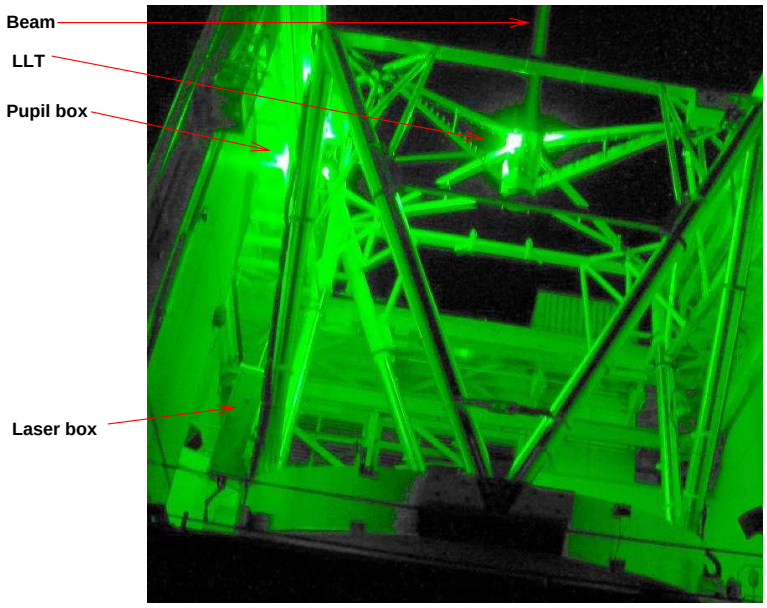

Figure 2: The Rayleigh LGS system at MMT, as viewed from outside of the dome. The beam path from the laser box to the LLT is in the air.

other systems and is close to optimum [11].

3 Design studies of the LGS sub-system

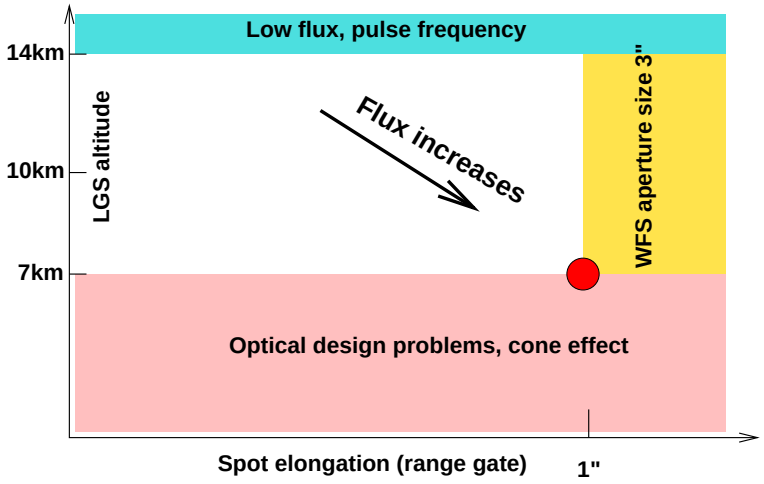

Figure 3: Trade space of the SAM LGS parameters – spot distance from the telescope (altitude) H and spot elongation α. The red circle depicts chosen parameters.

The design of the SAM LGS system is a result of several trade studies. Here, a brief summary is

given with references to more detailed documents. Constraints on the LGS altitude and spot elongation are illustrated in Fig. 3. The WFS field of view is 3″ square, limiting the allowable spot elongation.

3.1 LGS altitude

The SAM LGS can be placed at a distance (range) H from 7 km to 14 km. This distance will not be changed during SAM operation, but can, in principle, be re-adjusted during daytime. In the following, we call H "LGS altitude" for brevity. Selecting a higher altitude improves the compensation quality on-axis (less cone effect) but degrades compensation uniformity over the field. A lower altitude gives more uniform compensation and higher return flux (less laser power needed). By selecting a lower altitude, we also increase the chance of operating SAM with thin cirrus clouds located *above* the LGS.

The upper 14-km limit of the range is set by decreasing air density and the lowest pulse frequency of affordable industrial lasers. At higher ν_{PRF}, the pulse energy is less (for a given average power), making the laser cheaper. The lower limit of 7 km is dictated by the SAM optical design, because for lower altitudes the return laser beam in the SAM re-imaging system becomes too divergent. The WFS optical design delivers reasonable image quality over the whole 7–14 km range without changing the optics, only some re-adjustment is needed [20].

Originally, we expected the LGS to be placed at 10 km, in the middle of the range. After the study of the Pockels cell shutter, we prefer the lowest altitude of 7 km to reduce the impact of the ringing. A change of H still remains a possibility, if required by the SAM science.

3.2 Return flux

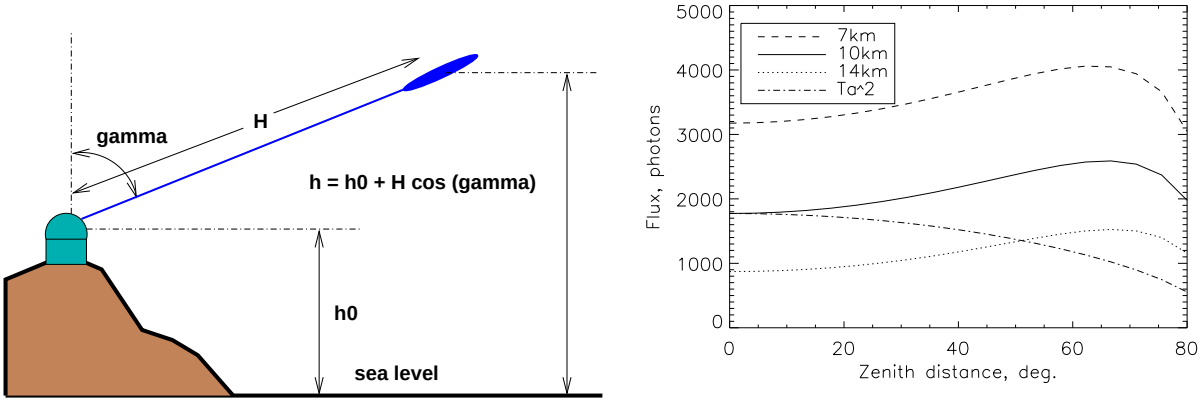

Figure 4: **Left:** Geometry of the laser spot in the atmosphere for observations at zenith angle γ from an observatory located at h_0 above the sea level. The air density at the spot depends on its altitude $h = h_0 + H\cos\gamma$. **Right:** Return flux expected for each SAM sub-aperture as a function of the zenith distance γ for three altitudes H and loop time 4.3 ms. Laser power 10 W, spot elongation 1″, system efficiency 0.087. The dash-dot line indicates the atmospheric absorption factor T_A^2 on the way up and down caused by Rayleigh scattering and aerosol optical depth $\tau_a = 0.11$.

The physics of Rayleigh scattering is well established and confirmed by the practice of LIDAR [2].

The return flux can thus be reliably estimated using the lidar equation. This calculation has been done for SAM [14]. However, in real astronomical systems the received flux is several times less than expected (cf. Table 1 in [14]), so making a reliable prediction is non-trivial.

In calculating the return flux for SAM (Fig. 4), we carefully and pessimistically estimated the transmission of the laser projector (0.71), SOAR telescope (0.45), SAM module (0.605), and WFS (0.64). The CCD quantum efficiency is 0.70 according to the manufacturer. The overall system efficiency at 355 nm is thus 0.087. This is similar to other LGS systems (0.09 at SOR, 0.11 at MMT).

Atmospheric absorption in the UV on the way up and down seriously reduces the number of returned photons and partially offsets the λ^{-3} gain from working in the UV. As the zenith distance γ increases, so does the absorption. However, at lower altitudes the air density is higher (we keep the range fixed, the altitude above sea level is $h = h_0 + H\cos\gamma$, where $h_0 = 2.7\,\mathrm{km}$ for Cerro Pachón). The net result is an increase of the flux away from the zenith up to $\gamma = 60°$ (the working limit for SAM). We included aerosol absorption with one-way optical depth of $\tau_a = 0.11$. The calculation in Fig. 4 is done for the spot elongation of $1''$ (range gate 119 m at $H = 7\,\mathrm{km}$) and laser power 10 W.

How many detected photons per spot N_{ph} do we actually need? The error budget allocates a certain error of adaptive-optics loop which can be related to the centroid error in the WFS and then to N_{ph}. However, this relation is not straightforward because many additional parameters intervene, such as spot size and elongation, wind speed, etc. [15]. Roughly, the SAM system will work correctly with $N_{ph} > 300$. It may be inferred from Fig. 4 that for $H = 7\,\mathrm{km}$ the power margin reaches 10, whereas it is only 3 for $H = 14\,\mathrm{km}$. Considering that the difference between the actual and estimated return flux in real AO systems may reach a factor of 10 [14] and that we may want to use $H = 14\,\mathrm{km}$, the actual choice of 10 W laser power does not appear excessive.

D. Sandler writes: *"We note that while 4 W of [sodium] laser power is very robust on paper, in reality it is extremely desirable to have more power. A factor of two margin will allow the LGS AO system to operate off zenith and for worse seeing. [...] The goal of the LGS AO developers should be to produce enough power to make the system flexible and robust, with the constraint that astronomers using the system should have to pay no attention to the laser"* ([4], p. 327).

The fast shutter of SAM transmits only polarized light. The laser light is polarized and the Rayleigh scattering preserves polarization, so it is, in principle, possible to design a LGS system without polarization losses. However, the LGS projector and SAM module with WFS rotate relative to each other. We plan to adjust the polarization of the emitted beam to obtain a circularly polarized return light at the entrance of SAM, to be transformed again to linear polarization by a $\lambda/4$ plate in the WFS. Some polarization losses will be inevitably incurred, of course. Aerosol scattering does not preserve polarization, so SAM will use only 1/2 of the flux scattered be aerosols. However, we have not included any aerosol scattering in our calculation of the return flux, which will be increased by the aerosol, compared to a pure Rayleigh scattering.

3.3 Fast shutter

Fast range-gating of the laser return signal can be done with a special CCD detector with "substrate shutter". This option is used in the MMT laser system, but it was rejected for SAM to avoid a special, single-source CCD. Instead, we employ a more traditional optical shutter based on a Pockels cell (Fig. 5; see [19]).

The short gating pulse excites acoustic oscillations in the piezo-electric KD*P crystal, causing

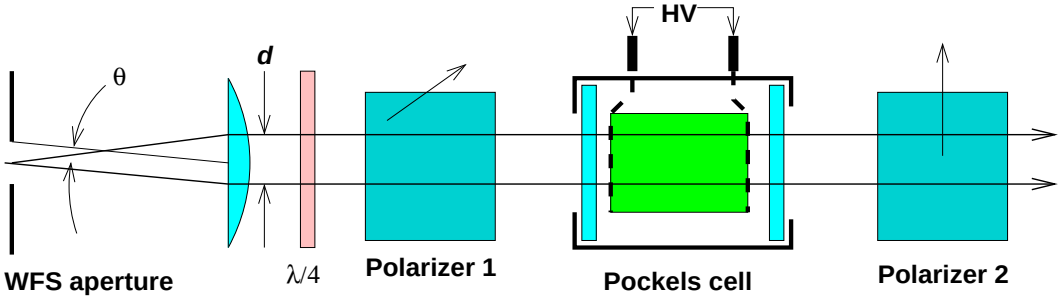

Figure 5: Pockels-cell shutter. An electro-optic crystal KD*P is placed between crossed polarizers. No light is transmitted until a voltage is applied during the range gate time Δt. The light entering the shutter is converted from circular to linear polarization by the $\lambda/2$ plate.

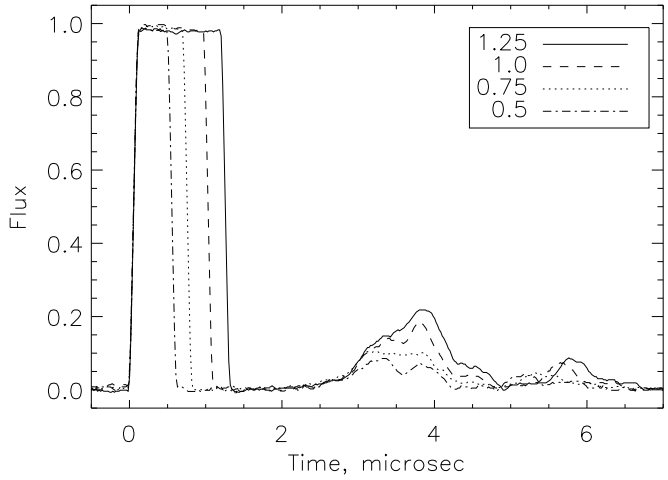

Δt, μs	$f = I_2/I_1$	Delay, μs
0.5	0.19	3.49
0.7	0.20	3.54
1.0	0.19	3.63
1.25	0.21	3.72

Figure 6: Light pulse transmitted through QX1020 Pockels cell with crossed polarizers, He-Ne laser, 4 kV pulse amplitude, for varying length of the drive pulse (in μs). The relative intensity and delay of the ringing after-pulse are listed in the table.

unwanted phase shifts, "ringing". We studied commercially available cells and selected QX1020 from Cleveland Crystals for its reportedly low ringing. The ringing phenomenon was understood and modeled quantitatively [21]. It turns out that for this specific cell, oscillations in the first resonance are acceptably low. For the short pulse durations encountered in SAM, the ringing is dominated by an after-pulse that comes 3.5 μs after the shutter opening and has a relative energy of 20% compared to the main pulse, independently of the range gate duration Δt (Fig. 6).

If after-pulses are unavoidable, their effect can be diminished by putting LGS at $H = 7$ km. At this altitude, the ringing after-pulses are sufficiently separated spatially from the main pulse and fall outside the WFS aperture for all spots, except the innermost ones. Mathematical modeling of elongated spots shows that the after-pulses are visible in the inner sub-apertures (Fig. 7). The shifts

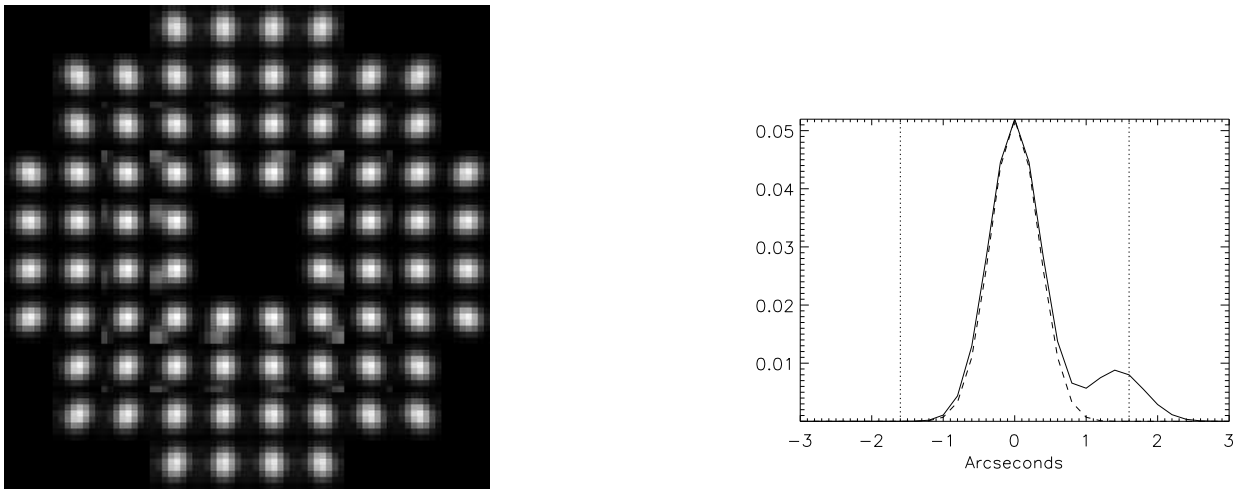

Figure 7: Images of all simulated spots for seeing FWHM $\epsilon = 1''$ (left) and cuts through the spot in the inner sub-aperture in the radial (full line) and tangential (dash) directions for the seeing $0.8''$, $\Delta t = 1\,\mu$s and $H = 7\,$km.

of the spot centroids caused by ringing were quantified by assuming an optimally weighted centroid algorithm where the influence of the after-pulse is reduced by a proper choice of the pixel weights. Neither weighting nor thresholding cannot eliminate the effect completely because the main spot and after-pulse partially overlap. The error depends on the seeing (i.e. spot size), going from 9 mas at $0.8''$ to 87 mas at $1.6''$. We will have to introduce small seeing-dependent corrections to the reference centroid positions in inner sub-apertures to counter-act the ringing.

3.4 Range gate and spot elongation

We can set such a short range gate Δt that the spots in the WFS are not elongated even in the outer-most sub-apertures. Increasing Δt, we gain proportionally in the number of photons, until the elongation starts to degrade the performance again. So, there is an optimum elongation. The first study has shown that the optimum choice of Δt corresponds to rather elongated spots [12]. This study has been repeated with a refined model of noise and more realistic input parameters and gave the same result [15]. Even with spot elongation of $4''$ the optimum is not yet reached and the performance still improves with increasing Δt.

Practically, the spot elongation is limited by the size of the WFS aperture, $3''$. We tentatively set the elongation to $1''$, to leave room for the atmospheric jitter of spots and their offsets caused by static aberrations. Hence, the duration of the range gate pulse will be $0.8\,\mu$s for $H = 7\,$km. The elongation can be easily changed during SAM operation.

3.5 Spot jitter

Spot positions in the WFS sub-apertures depend on the residual aberrations and tilt. The tilt is created by atmospheric turbulence on the way up (from LLT to the spot) and down. In some LGS AO systems, the tilt is eliminated by a fast up-link servo that aims the LLT beam in response to the WFS

and maintains the spots always centered. In SAM, we have chosen to eliminate the uplink tilt servo for simplicity and will compensate only slow tilt components with an update frequency of $\sim$1 Hz.

The rms atmospheric tilt is estimated by the formula $\sigma^2 = 0.17(\lambda/D)^2(D/r_0)^{5/3}$. The tilt is achromatic. In case of SAM, it is created by the ground-layer seeing only. Assuming the GL seeing of $1''$ and $D = 0.3$ m, we obtain $\sigma = 0.35''$. Spot excursions by $\pm 2\sigma = \pm 0.7''$ will be frequent. This is still acceptable with a $3''$ WFS field. With intrinsic spot width of $1''$, the elongation of $1''$ is barely perceptible even in the outer sub-apertures (Fig. 7) and still leaves enough room for the spot jitter and offsets needed to compensate for the non-common-path aberrations.

4 Laser selection

We identified two Q-switched industrial UV lasers potentially suitable for SAM, from *Photonics Industries*[2] and *JDSU*[3]. Both are frequency-tripled Nd:YAG lasers emitting at $\lambda = 355$ nm in a single TEM00 mode. Their parameters are listed in Table 3. The quotations from both vendors were obtained in March 2006 and specific questions related to the suitability of their lasers for SAM were asked. We also obtained references to customers using these lasers and quotations for de-scoped lasers of lower power. Each manufacturer claims to have produced tens if not hundreds of such lasers, mostly for material processing. Each laser is discussed below separately.

Table 3: Parameters of two UV lasers.

Parameter	Photonics	JDSU
Laser model	DS20-355	Q301-HD
Average power at $\nu_{PRF} = 10$ kHz, W	8	10
Pulse width, ns	40	34
Beam diameter, mm	0.9	0.26
Beam divergence, mrad	1.3	1.8
Beam stability, μrad	< 50	< 50
Beam quality M^2	< 1.1	< 1.2
Cost, kUSD	115	110
Laser head size,mm	600x191x127	813x127x86
Laser head weight, kg	17	14.5
MTBF, oper. hours	8000-10000	10000
Laser electronics power, W	<2200	400 typ.
Chiller power, W	< 2200	700 typ.
Working temp. range, °C	15-30	15-35
Umbilical cable length, m	3	≤ 7
Power supply size (mm) and mass (kg)	483x476x133, 17	427x364x76, 8.4
Chiller size (mm) and mass (kg)	483x432x178, 20	533x440x264, 55

[2]http//www.photonix.com
[3]http://www.jdsu.com

Photonics laser was our initial choice. The pump diodes (primary cause of failure) are connected to the laser cavity by fibers and are easily replaceable (diode cost $7600). The DS20 laser can have a widely variable ν_{PRF} and has regulated output power without degradation of the beam parameters. Power attenuation does not extend laser lifetime.

The company was consulted by our colleagues from the Michigan State University. As a result, a project of a specialized laser for SAM was outlined in 2003, but it has not been supported by the NSF AODP program. In this laser, the pump diodes would be located in some convenient place, while the laser head will be at the telescope top end, connected to the diodes by long fibers (as the GLAS laser). However, the heat generated in the laser head is still non-negligible (∼30%) and must be removed by a liquid coolant.

The manufacturer says that another potential cause of laser failure is the environment (dust, dirt, particles). The Photonics laser delivered to the University of Arizona (not DS20, other model) operated well in the laboratory but failed at the telescope because its frequency tripling crystal was affected by humidity. It seems that the DS20-355 laser can work in arbitrary orientation, although the manufacturer offers additional tests to verify this. The laser is warranted for 1 yr after purchase or 5000 h of operation.

In addition to the laser, the system contains the electronics unit and a compact solid-state chiller with air-cooled heat sinks. The total power consumption of both units is < 2200 W, no separate data on the typical consumption of each unit are given.

JDSU (former Lightwave) laser is our preferred choice. Two frequency-doubled lasers from this supplier have worked at MMT for several years without trouble, in a variable-gravity environment. The manufacturer confirms that gravity does not matter and that a non-operating laser withstands brief shocks up to 18g. The laser is warranted for 5000 operating hours or 13 months after shipment, whichever occurs first, but the MTBF is 10000 hours operation or 40 months of service.

There are no serviceable parts in the laser, its pumping diodes cannot be changed. It is not recommended to lower the laser power, and there is no gain in the laser lifetime in doing so. When the laser fails, it must be replaced by a new one.

The laser connects to its electronics by an umbilical cable (max. length 7 m) and to the chiller by a pair of hoses. The chiller is rather bulky and works only in the horizontal orientation. It has an air radiator.

Some other vendors offer UV Q-switched lasers which are not suitable for SAM for various reasons.

- Avia lasers from *Coherent* deliver suitably high power only for $\nu_{PRF} > 20$ kHz.
- Hawk-II from *Quantronix* can emit 5 W at $\nu_{PRF} = 20$ kHz. Not enough information on the web.
- *Continuum* sells flash-lamp powered UV lasers. This is an old and rather inefficient technology.

5 Beam transfer and LLT

The SAM LGS system must project a spot as small as possible to the desired altitude in the range 7–14 km. The optimum LLT diameter of 30 cm has been determined in [11] for $\lambda = 355$ nm and matches the 50-cm LLTs used by other groups for projecting visible-light LGS. The radius of the Gaussian

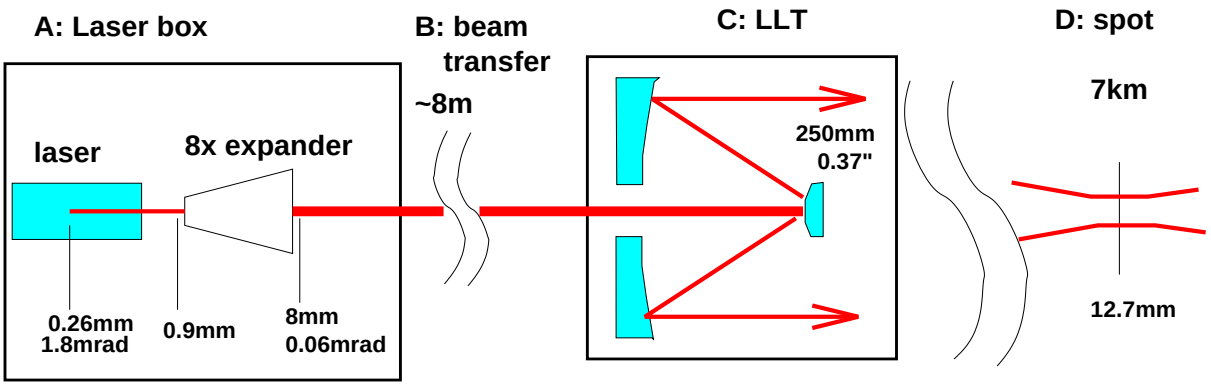

Figure 8: Path from the laser to the LLT. The beam diameter $2w$ and divergence 2θ (both at $1/e^2$ level) are indicated.

beam footprint on the LLT primary must be about w_1 =0.11–0.13 m (at $1/e^2$ level), depending on the seeing [11].[4] We do not plan to adjust this radius in response to changing conditions.

Both GLAS and MMT use refractive LLT designs. Their advantage is a sealed tube (less prone to optics contamination) and a generous tolerance on the lens flexure. However, the space and mass allocations for the SAM LLT are quite tight because the SOAR telescope has a smaller, light-weight secondary assembly. We developed initially a crude refractive LLT concept and discarded it in favor of a reflective design with a fast and light-weighted primary mirror [17]. The mechanical design of the LLT fulfilling all requirements (except mass) has been developed by A. Montané [23].

The optical design of a reflective LLT is trivial because we do not require a large field. An elliptical primary and a small spherical secondary mirror appear to be a logical choice. The size of the secondary is a free parameter in the design. We could use a very small secondary and illuminate it directly by a laser beam transmitted via several flat-mirror reflections. This strategy is adopted by the MMT (they use refractive LLT and expand the beam with lenses inside it). We have chosen to expand the beam by a moderate factor (8x) before launching it upwards to the LLT. This adds a degree of flexibility (now we can adjust the beam radius w_1) and reduces the beam intensity in the transport system (less prone to burning optics). The optical diameter of the LLT secondary mirror M2 is chosen to be 10 mm (optical magnification of the LLT 30x), but can be further optimized.

A schematic representation of the laser path to LLT (beam transfer optics, BTO) is shown in Fig. 8. The beam expander and other auxiliary optics are located in the thermo-stabilized and closed *laser box*. A quasi-parallel beam is then directed towards the LLT by reflections from 2 flat mirrors. The beam path is enclosed in aluminum tubes to protect it from dust and as a safety feature, in case of a failure to direct the beam properly.

6 SAM LGS at SOAR

Interfacing the SAM LGS system with SOAR is a critical aspect for SAM, and for SOAR as well because the telescope performance must not be adversely affected by the installation of the laser.

[4]The FWHM is 1.177 times w, or 0.13–0.15 m

6.1 Location of the LGS sub-system

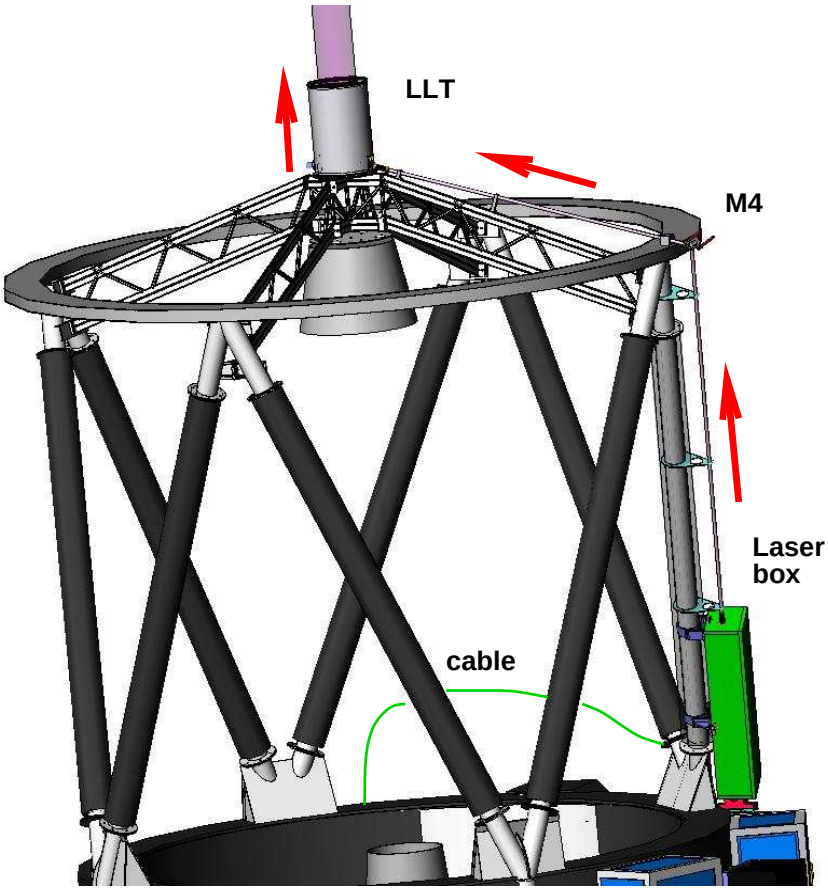

Figure 9: Beam transport from the laser box to the LLT.

The LLT position behind the SOAR secondary mirror is pre-determined by the requirement for proper SAM operation. In principle, the LLT could be located on the side of the aperture (like the laser telescope at Keck), but this would require doubling the number of expensive laser photons for compensating larger spot elongation with a shorter range gate. Even worse, the spot elongation pattern will be fixed with respect to the SOAR structure, but will rotate w.r.t. the SAM WFS as the Nasmyth bearing rotates to compensate for parallactic angle. Thus, the loop control becomes much more complicated and we will likely get a PSF with a rotating asymmetry as a result.

The laser position can be chosen freely on the SOAR tube. The whole system will point together with the SOAR, otherwise a complicated pointing to direct the beam to the LLT would be required. After considering several options, it has been decided to place the laser box on the truss above the unused bent-cassegrain port #2, at position angle 45° from the IR Nasmyth (Fig. 9). An alternative laser location on the other side of the elevation ring (or truss) was considered, but this space is heavily used for the SOAR service (mirror washing etc.).

The laser will be looking “up”. A beam will emerge from the laser box along the truss. It will be

intercepted by the flat mirror M4 and directed to the LLT. The beam path will be enclosed in two protective tubes. The mirror M4 will be remotely controlled in tilts to facilitate alignment and, if necessary, to compensate the flexure actively.

6.2 Location of the laser electronics and cooler

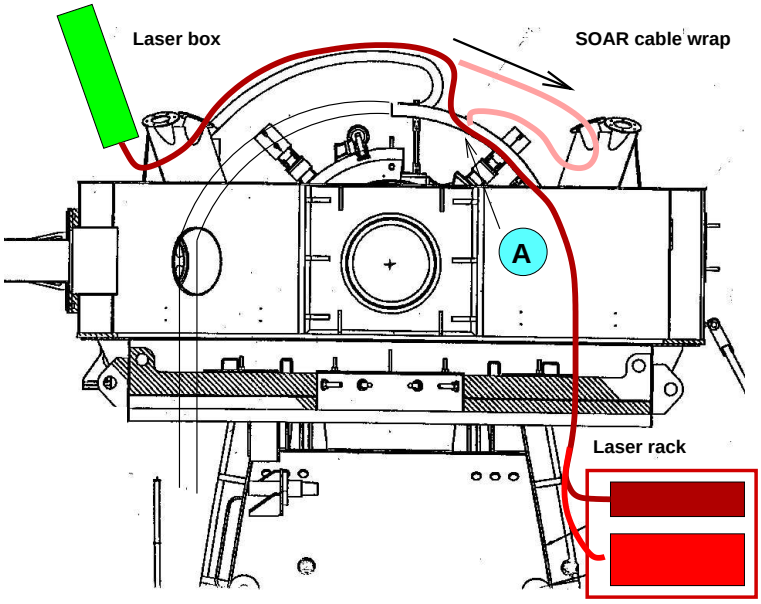

Figure 10: Suggested cable path from the laser to its cooler and electronics installed in a thermal rack.

The length of the laser electric umbilical cable and cooling lines can be chosen between 3 m and 5 m, JDSU delivers also 7 m cable as a standard. Our question whether either umbilical or cooling lines could be extended beyond 7 m was answered negatively by JDSU[5] and not answered at all by Photonics.

We considered several potential placements for the laser cooler and the laser box itself. Finally, it was decided that the cooler and electronics will be located in a thermal rack attached to the side of the elevation pillow opposite to the cable wrap. The laser cable will pass through the initial section of the normal SOAR cable wrap (on the IR side) and then goes down directly to the cabinet, as shown in Fig. 10.

6.3 SOAR flexure

Flexure of the SOAR truss affects the beam path from the laser box to the LLT and the LLT pointing. The specifications for SOAR are M2 displacement of less than 0.5 mm and tilt of less than 15″ for

[5] Jonathann King wrote on December 21, 2006: "The maximum standard umbilical length is 7 m. We could probably stretch this to 10 m with a custom umbilical, but this would require some testing. [...] Again, our standard limit [of the cooling-hose line] is 7 m, but we may be able to stretch this to 10 m. Special engineering would be required. Anything more that 10 m would definitely require custom software development to keep the control loops stable."

elevation change from zenith to horizon. These specifications are actually met[6]. D. Neill has studied the flexture of the SOAR optical support structure (OSS) in July 2007 and determined that the displacement and tilt of M2 relative to M1 are 0.23 mm and 3.7″, respectively, for the elevation change from zenith to horizon.

By installing the LLT mass on top of the M2 assembly and the laser box on the truss, we add the load and may adversely affect the SOAR performance. The study of D. Neill has shown that these effects are negligibly small, resulting in the M2 displacement and tilt changes of less than 37 μm and 0.7″ respectively. In case of the LLT, this negligible effect has been confirmed by direct measurements on the telescope conducted with and without 14-kg LLT dummy mass. Thus, the initial LLT mass budget of 8 kg was over-constrained and even its design mass of 14 kg has no effect on SOAR.

It is expected that the LGS projection system will not be significantly affected by the flexture of the SOAR OSS. The $1/e^2$ beam diameter on the LLT M2 mirror is 8 mm. If the flexure sag of 0.23 mm causes a similar displacement of the beam on M2, it is only 2.6% of the beam diameter and can be left uncorrected. The actual displacement may be larger because both laser box and M4 will be afected by the flexute of the SOAR structure. As a precaution, we implement active control of the laser beam by the tilts of M4, so that the illumination of the LLT primary mirror can be always symmetric.

The changes of the laser beam angle caused by flexure can be neglected on the path from the laser box to the LLT because the LLT has an optical magnification of 32x. Thus, to cause a beam shift of 1″ on the sky, the angle of the input beam must change by 32″ – much larger than the actual tilts caused by the flexure. Only the tilts of the LLT as a whole with respect to the SOAR optical axis matter. The tilt of the SOAR M2 assembly (which holds the LLT) has been measured during experiments in May 2007. We placed a point source on the optical axis of SOAR (at the rotation center of the Nasmyth focus) and measured the beam deflection by a system attached to the SOAR M2. With the SOAR active optics working, the relative tilt does not exceed ±5″ for elevation change from zenith to 30°. Thus, we are confident that the orientation of the LLT axis relative to SOAR will be kept nearly constant. Residual small tilts can be removed by correcting the LLT pointing with a look-up table. Some LLT tilts will be caused also by changing temperature. During commissioning, we will study the LLT tilts relative to SOAR by observing bright stars with a boresight camera in the LLT.

6.4 Electric connections

Essentially all electronic components of the SAM LGS system will be procured commercially, hence there is no need for in-house development. Figure 11 shows various connections between the elements of the SAM LGS and to the outside world. Most remotely controlled motions will communicate through RS232 lines.

6.5 Other issues

Safety of the SAM LGS system is addressed in a separate document [10]. It will be safe to work inside the dome with the LGS emitting into the sky. Even in the event when the laser beam is directed to the dome wall and scattered back, the people inside the dome are safe. The LGS is designed to be safe in case of a single-mode failure. For this reason the narrow and dangerous laser beam on its way up to the LLT is enclosed in protective tubes. The 355 nm UV radiation does not present

[6] V. Krabbendam, private communication

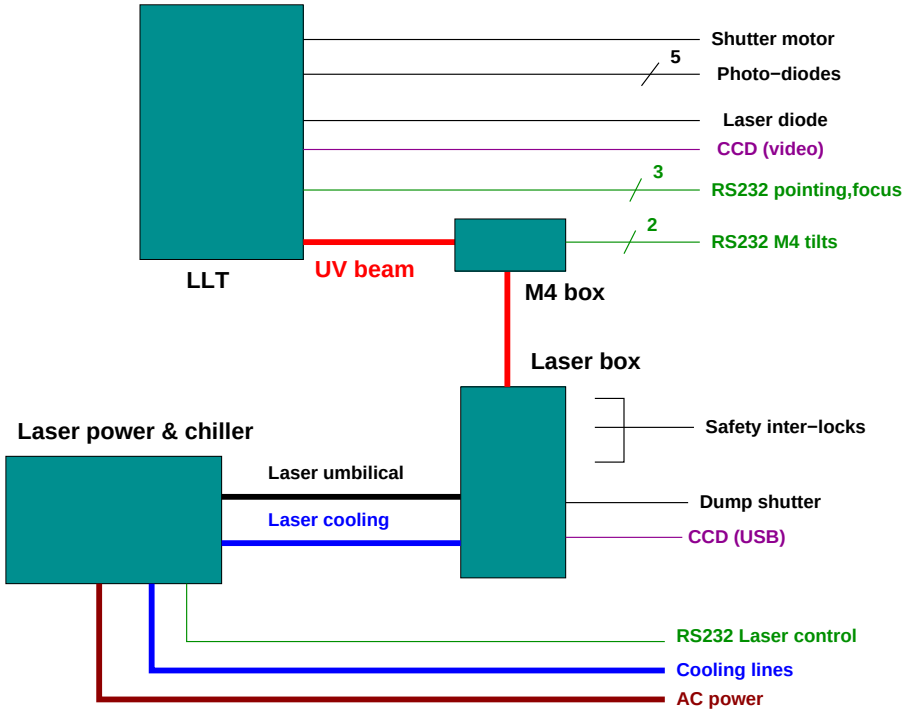

Figure 11: Top-level connections of the SAM LGS system.

visual and photo-chemical hazards. The SAM laser beam is safe for airplanes, no human spotters are needed. However, the maintenance and initial setup of the LGS system do present a hazard and will be performed only by qualified personnel with suitable precautions and procedures to minimize the risk.

Access to the equipment installed at the truss and on the top end of the SOAR tube is difficult. It requires the use of the man-lift with all associated overheads and restrictions. The SAM LGS system must be designed to minimize the need of access for service, maintenance, and diagnostic. Remote diagnostics will reduce the effort required for operating and maintaining SAM LGS.

References

[1] Baranec, C., Lloyd-Hart, M., Milton, N., Stalcup, T., Snyder, M., Angel, R., "Tomographic reconstruction of stellar wavefronts from multiple laser guide stars", *Proc. SPIE,* **7272**, paper 3, 2006.

[2] Hardy, J.W., "Adaptive Optics for Astronomical Telescopes", Oxford Univ. Press, NY, 1998

[3] V.L. Krabbendam, T.A. Sebring, and S. Heathcote, "Southern Astrophysical Research Telescope (SOAR): steps on the road to success", *Proc. SPIE,* **4837**, pp. 71-81, 2003.

[4] Roddier F. (ed.) Adaptive optics in astronomy. Cambridge Univ. Press, 1999.

[5] R.G.M. Rutten, P. Clark, R.M. Myers et al., "Facility class Rayleigh beacon AO system for the 4.2-m William Hershel Telescope", *Proc. SPIE,* **4839,** pp. 360-369, 2003.

[6] A. Tokovinin, B. Gregory, H. Schwarz, "Visible-light AO system for the 4.2-m SOAR telescope", *Proc. SPIE,* **4839,** pp. 673-680, 2003.

[7] A. Tokovinin, "Seeing improvement with ground-layer adaptive optics", *Publ. Astron. Soc. Pacif.,* **116**, pp. 941-951, 2004

[8] A. Tokovinin, S. Thomas, B. Gregory, N. van der Bliek, P. Schurter, R. Cantarutti, E. Mondaca, "Design of ground-layer turbulence compensation with a Rayleigh beacon", *Proc. SPIE,*, **5490**, pp. 870-878, 2004.

System design notes:

[9] Functional and performance requirements of SAM. October 26, 2005.

[10] SAM-AD-02-0004, "Laser safety of SAM", January 31, 2007

[11] SAM-AD-02-1105, "Laser Launch Telescope Diameter and Return Flux" May 14, 2004

[12] SAM-AD-02-1106, "Optimum spot elongation in SAM", February 16, 2005

[13] SAM-AD-02-1109, "SAM error budget", May 26, 2005

[14] SAM-AD-02-1112, "Calculation of the laser return flux", February 2, 2006

[15] SAM-AD-02-1113, "SAM optimization: part II", June 8, 2007

[16] SAM-AD-02-1114, "Requirements for the SAM LGS system", May 8, 2006

[17] SAM-AD-02-2102, "Reflective laser launch telescope for SAM", May 9, 2006

[18] SAM-AD-02-2101, "Concept of the LGS beam transfer and beam control", May 8, 2006

[19] SAM-AD-02-2208, "Fast shutter with Pockels cell", July 4, 2006

[20] SAM-AD-02-2209, "SAM WFS Design", July 12, 2006

[21] SAM-AD-02-2308, "Testing the Pockels cell shutter", November 8, 2006

[22] SAM-AD-02-2309, "SAM LGS Laser Box, Controller and Chiller Location", December 29, 2006

[23] SAM-AD-02-3209, "Mechanical design of the laser launch telescope", June 11, 2007

[24] SAM-AD-02-6301, "SOAR flexure tests", May 9, 2007